

On the discontinuous Galerkin method for the numerical solution of the Navier–Stokes equations ^{*}

Vít Dolejší[†]

Charles University Prague, Faculty of Mathematics and Physics, Sokolovská 83, 186 75 Praha, Czech Republic, dolejsi@karlin.mff.cuni.cz

Abstract

The paper deals with the use of the discontinuous Galerkin finite element method (DGFEM) for the numerical solution of viscous compressible flows. We start with a scalar convection-diffusion equation and present a discretization with the aid of the nonsymmetric variant of DGFEM with interior and boundary penalty terms. We also mention some theoretical results. Then we extend the scheme to the system of the Navier-Stokes equations and discuss the treatment of stabilization terms. Several numerical examples are presented.

Keywords: compressible Navier-Stokes equations, discontinuous Galerkin finite element method, nonsymmetric variant of diffusion terms, interior and boundary penalty, method of lines

1 INTRODUCTION

Our goal is to develop a sufficiently accurate and robust method for the numerical solution of viscous compressible flows. During last years we have dealt with combined finite volume (FV) – finite element (FE) methods which give good results in many cases of technically relevant problems in complex domains. For analysis and applications, see, e. g., [2], [21], [22], [23], [24], [25]. However, their drawback is the necessity to construct two mutually associated meshes, which is rather complicated particularly in 3D, see [27]. Moreover, these schemes, which are only of the first order of accuracy, suffer from a high amount of numerical viscosity. For problems with a small physical viscosity, the numerical viscosity dominates and we cannot obtain satisfactory results. In order to avoid such difficulties, the application of a higher order scheme is necessary.

One possibility is to use higher order FV schemes based on a higher order reconstruction, e. g., TVD, ENO, WENO schemes, for their survey see [1], [32]. An alternative approach is a discontinuous Galerkin (DG) method, which is in fact a generalization of finite volume method (FVM) in the sense of Remark 3.1 in this paper. DG methods are based on piecewise polynomial approximations without any requirement on the interelement continuity. It uses only one mesh and gives higher order schemes. Recently, the DG method has become quite popular and it is discussed in a number of papers. For a survey about DG methods, see [8] or [9].

Various numerical experiments indicate that DG methods are particularly suitable for the numerical solution of nonlinear conservation laws with discontinuous solutions and nonlinear convection-diffusion problems whose solutions have steep gradients, see [9]. The use of DG method for the numerical simulation of compressible flows is not completely new. In 1997, Bassi and Rebay [5], [6] solved the Navier-Stokes equations with the aid of the mixed DG method, where a solution \mathbf{w} and its gradient $\nabla\mathbf{w}$ are considered as independent variables. In 1998, Lomtev, Quillen and Karniadakis [29] used the DG-space discretization method to deal with the convective part of the compressible Navier-Stokes equations and used a mixed method to approximate the diffusive part of the equations. In 1999, Baumann and Oden [7] introduced a *hp* discontinuous Galerkin finite element (DGFE) scheme, which was applied for the compressible Euler

^{*}This work was supported under the grants No. 201/02/0684 and No. 201/00/D116 of the Grant Agency of the Czech Republic and by the Grant MSM 113200007.

equations and proposed for the Navier-Stokes equations. Since the method is not a mixed method, it results in fewer degrees of freedom per element.

In this paper we propose a new method for the solution of the Navier-Stokes equations which is based on the nonsymmetric variant of DGFEM. The novelty of our approach is that unlike the Baumann-Oden method, we add to the scheme *interior and boundary penalty terms*. Such scheme was analyzed in [31] for elliptic problems. In [14] and [15] we extended this analysis to scalar nonlinear convection-diffusion problems. In [13], we applied DGFEM for the numerical solution of inviscid compressible flows. Here we extend DGFEM to the solution of viscous flows.

The contents of the paper are the following. In Section 2 we deal with the numerical solution of a scalar convection-diffusion equation with the aid of DGFEM. We present a numerical scheme and mention some theoretical results concerning a priori error estimates from [15]. In Section 3 we extend the numerical scheme to the systems of the Navier-Stokes equations. In order to employ the nonsymmetric variant of DGFEM for the Navier-Stokes equations, the viscous terms have to be linear with respect to $\nabla \mathbf{w}$. The treatment of stabilization diffusive terms is discussed. Several numerical examples are given in Section 4.

2 SCALAR CONVECTION-DIFFUSION EQUATION

We start with the numerical solution of a scalar equation. Following [14] and [15] we briefly derive a numerical scheme based on the DGFE discretization.

We use the standard notation for function spaces: $H^k(\Omega)$ = Sobolev space, $L^2(0, T; X)$ = Bochner space of square integrable functions on $(0, T)$ with values in a Banach space X , $C^1(0, T; X)$ = space of continuously differentiable mappings in $(0, T)$ with values in X .

2.1 Continuous problem

Let $\Omega \subset \mathbb{R}^d$ ($d = 2$ or 3) be a bounded polyhedral domain and $T > 0$. We set $Q_T = \Omega \times (0, T)$ and by $\partial\Omega$ we denote the boundary of Ω which consists of two disjoint parts $\partial\Omega_D$ and $\partial\Omega_N$. We consider the following *initial-boundary value problem*: Find $u : Q_T \rightarrow \mathbb{R}$ such that

$$\frac{\partial u}{\partial t} + \sum_{s=1}^d \frac{\partial f_s(u)}{\partial x_s} = \sum_{s=1}^d \frac{\partial R_s(u, \nabla u)}{\partial x_s} + g \quad \text{in } Q_T, \quad (1)$$

$$u(x, t) = u_D(x) \quad \text{for } x \in \partial\Omega_D, t \in (0, T), \quad (2)$$

$$\sum_{s=1}^d R_s(u, \nabla u) n_s = g_N \quad \text{for } x \in \partial\Omega_N, t \in (0, T), \quad (3)$$

$$u(x, 0) = u^0(x), \quad x \in \Omega. \quad (4)$$

Here $x = (x_1, \dots, x_d)$ and t denotes the space and time coordinates and $\mathbf{n} = (n_1, \dots, n_d)$ is a unit outer normal to $\partial\Omega$. We suppose that $f_s \in C^1(\mathbb{R})$, $R_s \in C^1(\mathbb{R}^{d+1})$, $R_s(u, \alpha)$ is linear with respect to $\alpha \in \mathbb{R}^d$.

Let $V = \{v; v \in H^1(\Omega), v|_{\partial\Omega_D} = 0\}$. We say that u is a *weak solution* of (1)–(4) if the following conditions are satisfied

$$\text{a) } u \in L^2(0, T; H^1(\Omega)), \quad u \in L^\infty(Q_T), \quad (5)$$

$$\text{b) } \frac{d}{dt}(u(t), v) + \int_{\Omega} \sum_{s=1}^d \frac{\partial f_s(u)}{\partial x_s} v \, dx + \int_{\Omega} \sum_{s=1}^d R_s(u, \nabla u) \frac{\partial v}{\partial x_s} \, dx - \int_{\partial\Omega_N} g_N v \, dS = (g(t), v)$$

for all $v \in V$ in the sense of distributions on $(0, T)$,

$$\text{c) } u = u_D \quad \text{on } \partial\Omega_D \text{ in the sense of traces,}$$

$$\text{d) } u(0) = u_0 \quad \text{in } \Omega.$$

By (\cdot, \cdot) we denote the L^2 -scalar product and by $u(t)$ the function on Ω such that $u(t)(x) = u(x, t)$, $x \in \Omega$.

The existence and uniqueness of the weak solution (5) a)–d) was shown in [23] for a special case of (1)–(4) with

$$\sum_{s=1}^d \frac{\partial R_s(u, \nabla u)}{\partial x_s} = \varepsilon \Delta u \quad (6)$$

and

$$\partial\Omega_N = \emptyset, \quad (7)$$

where $\varepsilon > 0$ is a given constant which plays a role of viscosity.

In the following we assume that the data are sufficiently regular so that there exists of a *strong solution*, i.e., a function u such that $u \in L^2(0, T; H^{p+1}(\Omega))$ and $\partial u / \partial t \in L^2(0, T; H^{p+1}(\Omega))$ for some $p > 1$, which satisfies (1)–(4) pointwise almost everywhere.

2.2 Discretization

Let \mathcal{T}_h ($h > 0$) denotes a partition of the closure $\bar{\Omega}$ of the domain Ω into a finite number of closed d -dimensional convex polyhedra K with mutually disjoint interiors. We call \mathcal{T}_h a triangulation of $\bar{\Omega}$, but *do not* require the usual conforming properties for the finite element method. In 2D problems we choose usually $K \in \mathcal{T}_h$ as triangles or quadrilaterals. In 3D, $K \in \mathcal{T}_h$ can be, e.g., tetrahedra, pyramids or hexahedra. We can allow even more general elements K .

We set $h_K = \text{diam}(K)$, $h = \max_{K \in \mathcal{T}_h} h_K$. By $|K|$ we denote the d -dimensional Lebesgue measure of K . All elements of \mathcal{T}_h will be numbered so that $\mathcal{T}_h = \{K_i\}_{i \in I}$, where $I \subset \mathbb{Z}^+ = \{1, 2, \dots\}$ is a suitable index set. If two elements $K_i, K_j \in \mathcal{T}_h$ contain a nonempty open face which is a part of a $(d-1)$ -dimensional hyperplane, we call them *neighbours*. We set in this case $\Gamma_{ij} = \partial K_i \cap \partial K_j$ and assume that the whole set Γ_{ij} is a part of a $(d-1)$ -dimensional hyperplane. For $i \in I$ we set $s(i) = \{j \in I; K_j \text{ is a neighbour of } K_i\}$.

The boundary $\partial\Omega$ is formed by a finite number of faces of elements K_i adjacent to $\partial\Omega$. We denote all these boundary faces by S_j , where $j \in I_b \subset \mathbb{Z}^- = \{-1, -2, \dots\}$ and set $\gamma(i) = \{j \in I_b; S_j \text{ is a face of } K_i\}$, $\Gamma_{ij} = S_j$ for $K_i \in \mathcal{T}_h$ such that $S_j \subset \partial K_i$, $j \in I_b$. For K_i not containing any boundary face S_j we set $\gamma(i) = \emptyset$. Obviously, $s(i) \cap \gamma(i) = \emptyset$ for all $i \in I$. Now, if we write $S(i) = s(i) \cup \gamma(i)$, we have

$$\partial K_i = \bigcup_{j \in S(i)} \Gamma_{ij}, \quad \partial K_i \cap \partial\Omega = \bigcup_{j \in \gamma(i)} \Gamma_{ij}. \quad (8)$$

Moreover, we define two subsets $\gamma_D(i)$ and $\gamma_N(i)$ corresponding to $\partial\Omega_D$ and $\partial\Omega_N$ parts of boundary, respectively. Obviously,

$$\gamma(i) = \gamma_D(i) \cup \gamma_N(i) \quad \text{and} \quad \gamma_D(i) \cap \gamma_N(i) = \emptyset. \quad (9)$$

Furthermore, we use the following notation: $\mathbf{n}_{ij} = ((n_{ij})_1, \dots, (n_{ij})_d) =$ unit outer normal to ∂K_i on the face Γ_{ij} , $d(\Gamma_{ij}) = \text{diam}(\Gamma_{ij})$, $|\Gamma_{ij}| = (d-1)$ -dimensional Lebesgue measure of Γ_{ij} .

Over the triangulation \mathcal{T}_h we define the *broken Sobolev space*

$$H^k(\Omega, \mathcal{T}_h) = \{v; v|_K \in H^k(K) \forall K \in \mathcal{T}_h\}. \quad (10)$$

For $v \in H^1(\Omega, \mathcal{T}_h)$ we introduce the following notation

$$\begin{aligned} v|_{\Gamma_{ij}} &= \text{the trace of } v|_{K_i} \text{ on } \Gamma_{ij}, \\ v|_{\Gamma_{ji}} &= \text{the trace of } v|_{K_j} \text{ on } \Gamma_{ji} = \Gamma_{ij}, \\ \langle v \rangle_{\Gamma_{ij}} &= \frac{1}{2} (v|_{\Gamma_{ij}} + v|_{\Gamma_{ji}}), \\ [v]_{\Gamma_{ij}} &= v|_{\Gamma_{ij}} - v|_{\Gamma_{ji}}. \end{aligned} \quad (11)$$

Obviously, $\langle v \rangle_{\Gamma_{ij}} = \langle v \rangle_{\Gamma_{ji}}$, but $[v]_{\Gamma_{ij}} = -[v]_{\Gamma_{ji}}$ and $[v]_{\Gamma_{ij}} \mathbf{n}_{ij} = [v]_{\Gamma_{ji}} \mathbf{n}_{ji}$.

The approximate solution of problem (1)–(4) is sought in the space of discontinuous piecewise polynomial functions

$$S_h = S^{p,-1}(\Omega, \mathcal{T}_h) = \{v; v|_K \in P_p(K) \forall K \in \mathcal{T}_h\}, \quad (12)$$

where $P_p(K)$ denotes the space of all polynomials on K of degree $\leq p$.

In order to derive the discrete problem, we start from a strong solution u such that $u \in L^2((0, T), H^2(\Omega))$ and $\frac{\partial u}{\partial t} \in L^2((0, T), H^2(\Omega))$. We multiply equation (1) by any $\varphi \in H^2(\Omega, \mathcal{T}_h)$, integrate over $K \in \mathcal{T}_h$, apply Green's theorem and sum over all $K \in \mathcal{T}_h$. Moreover, we use the relations $\langle \nabla u \rangle_{\Gamma_{ij}} = \nabla u|_{\Gamma_{ij}} = \nabla u|_{\Gamma_{ji}}$ and the identities

$$\int_{\Gamma_{ij}} \sum_{s=1}^d \langle R_s(u, \nabla \varphi) \rangle (n_{ij})_s [u] \, dS = 0, \quad \int_{\Gamma_{ij}} [u] [\varphi] \, dS = 0 \quad \forall j \in s(i) \quad \forall i \in I. \quad (13)$$

Furthermore, adding some terms which mutually cancel, we find that

$$\begin{aligned}
\int_{\Omega} \frac{\partial u}{\partial t} \varphi \, dx &+ \sum_{i \in I} \left\{ \sum_{j \in S(i)} \int_{\Gamma_{ij}} \sum_{s=1}^d f_s(u) (n_{ij})_s \varphi|_{\Gamma_{ij}} \, dS \right. \\
&- \int_{K_i} \sum_{s=1}^d f_s(u) \frac{\partial \varphi}{\partial x_s} \, dx + \int_{K_i} \sum_{s=1}^d R_s(u, \nabla u) \frac{\partial \varphi}{\partial x_s} \, dx \\
&- \sum_{\substack{j \in S(i) \\ j < i}} \int_{\Gamma_{ij}} \sum_{s=1}^d \left(\langle R_s(u, \nabla u) \rangle (n_{ij})_s [\varphi] - \langle R_s(u, \nabla \varphi) \rangle (n_{ij})_s [u] \right) \, dS \\
&- \sum_{j \in \gamma_D(i)} \int_{\Gamma_{ij}} \sum_{s=1}^d \left(R_s(u, \nabla u) (n_{ij})_s \varphi - R_s(u, \nabla \varphi) (n_{ij})_s (u - u_D) \right) \, dS \\
&+ \left. \sum_{j \in S(i)} \int_{\Gamma_{ij}} \sigma[u] [\varphi] \, dS + \sum_{j \in \gamma_D(i)} \int_{\Gamma_{ij}} \sigma(u - u_D) \varphi \, dS \right\} \\
&= \int_{\Omega} g \varphi \, dx + \sum_{i \in I} \sum_{j \in \gamma_N(i)} \int_{\Gamma_{ij}} g_N \varphi \, dS.
\end{aligned} \tag{14}$$

Here σ is a weight function defined on each Γ_{ij} by $\sigma|_{\Gamma_{ij}} = \varepsilon/d(\Gamma_{ij})$, where $\varepsilon \approx R_s$. Let us note that the form (14) represents a *nonsymmetric variant* of DGFEM since the *stabilization terms*

$$\begin{aligned}
&\sum_{\substack{j \in S(i) \\ j < i}} \int_{\Gamma_{ij}} \sum_{s=1}^d \langle R_s(u, \nabla u) \rangle (n_{ij})_s [\varphi] \, dS, \\
&\sum_{\substack{j \in S(i) \\ j < i}} \int_{\Gamma_{ij}} \sum_{s=1}^d \langle R_s(u, \nabla \varphi) \rangle (n_{ij})_s [u] \, dS
\end{aligned} \tag{15}$$

and

$$\begin{aligned}
&\sum_{j \in \gamma_D(i)} \int_{\Gamma_{ij}} \sum_{s=1}^d R_s(u, \nabla u) (n_{ij})_s \varphi \, dS, \\
&\sum_{j \in \gamma_D(i)} \int_{\Gamma_{ij}} \sum_{s=1}^d R_s(u, \nabla \varphi) (n_{ij})_s u \, dS
\end{aligned} \tag{16}$$

have opposite signs. This stabilization technique was proposed in [4] and [7] for diffusion and convection-diffusion problems, respectively and studied in [30]. The advantage of this approach is that the corresponding diffusive bilinear form has a favorable coercivity property, see the analysis in [4], [15], [30].

The adding the *interior penalty terms* $\int_{\Gamma_{ij}} \sigma[u] [\varphi] \, dS$, $j \in S(i)$ arises from the observation that just as Dirichlet boundary conditions can be imposed weakly instead of being built into the finite element space as in [3], so interelement continuity could be obtained in a similar fashion. Terms $\int_{\Gamma_{ij}} \sigma[u] [\varphi] \, dS$, $j \in \gamma_D(i)$ represents the *boundary penalty* introduced in [3].

The nonsymmetric variant of DGFEM with interior and boundary penalty terms was analyzed in [31] for elliptic problems and in [14] we extended this analysis to nonlinear convection-diffusion problems.

Similarly as in FVM the inviscid fluxes will be approximated with the aid of the so-called *numerical flux* $H(u, u', \mathbf{n})$:

$$\int_{\Gamma_{ij}} \sum_{s=1}^d f_s(u) n_s \varphi \, dS \approx \int_{\Gamma_{ij}} H(u|_{\Gamma_{ij}}, u|_{\Gamma_{ji}}, \mathbf{n}_{ij}) \varphi \, dS, \quad i \in I, j \in S(i). \tag{17}$$

Of course, if $j \in \gamma(i)$ and $\Gamma_{ij} \subset \partial\Omega$, it is necessary to specify the meaning of $u|_{\Gamma_{ji}}$. Here we use the

extrapolation, i.e. we put $u|_{\Gamma_{ji}} := u|_{\Gamma_{ij}}$. In this way we obtain the convection form:

$$\begin{aligned} b_h(u_h, \varphi_h) &= \sum_{i \in I} \left(\sum_{j \in s(i)} \int_{\Gamma_{ij}} H(u_h|_{\Gamma_{ij}}, u_h|_{\Gamma_{ji}}, \mathbf{n}_{ij}) \varphi_h|_{\Gamma_{ij}} dS \right. \\ &\quad + \sum_{j \in \gamma(i)} \int_{\Gamma_{ij}} H(u_h|_{\Gamma_{ij}}, u_h|_{\Gamma_{ij}}, \mathbf{n}_{ij}) \varphi_h|_{\Gamma_{ij}} dS \\ &\quad \left. - \sum_{i \in I} \int_{K_i} \sum_{s=1}^d f_s(u_h) \frac{\partial \varphi_h}{\partial x_s} dx \right), \quad u_h, \varphi_h \in H^2(\Omega, \mathcal{T}_h). \end{aligned} \quad (18)$$

Now, for $u_h, \varphi_h \in H^2(\Omega, \mathcal{T}_h)$ we define the forms

$$\begin{aligned} a_h(u_h, \varphi_h) &= \sum_{i \in I} \left\{ \int_{K_i} \sum_{s=1}^d R_s(u_h, \nabla u_h) \frac{\partial \varphi_h}{\partial x_s} dx \right. \\ &\quad - \sum_{\substack{j \in s(i) \\ j < i}} \int_{\Gamma_{ij}} \sum_{s=1}^d \left((R_s(u_h, \nabla u_h)) (n_{ij})_s [\varphi_h] - \langle R_s(u_h, \nabla \varphi_h) \rangle (n_{ij})_s [u_h] \right) dS \\ &\quad \left. - \sum_{j \in \gamma_D(i)} \int_{\Gamma_{ij}} \sum_{s=1}^d \left(R_s(u_h, \nabla u_h) (n_{ij})_s \varphi_h - R_s(u_h, \nabla \varphi_h) (n_{ij})_s u_h \right) dS \right\}, \end{aligned} \quad (19)$$

$$J_h(u_h, \varphi_h) = \sum_{i \in I} \left\{ \sum_{j \in s(i)} \int_{\Gamma_{ij}} \sigma [u_h] [\varphi_h] dS + \sum_{j \in \gamma_D(i)} \int_{\Gamma_{ij}} \sigma u_h \varphi_h dS \right\}, \quad (20)$$

$$\begin{aligned} \ell_h(\varphi_h)(t) &= \int_{\Omega} g(t) \varphi_h dx + \sum_{i \in I} \left\{ \sum_{j \in \gamma_N(i)} \int_{\Gamma_{ij}} g_N \varphi_h dS \right. \\ &\quad \left. + \sum_{j \in \gamma_D(i)} \int_{\Gamma_{ij}} \sum_{s=1}^d \left(R_s(u, \nabla \varphi_h) (n_{ij})_s u_D(t) + \sigma u_D(t) \varphi_h \right) dS \right\}, \end{aligned} \quad (21)$$

$$(\alpha, \beta) = \int_{\Omega} \alpha \beta dx. \quad (22)$$

By $u(t)$ we denote the function on Ω such that $u(t)(x) = u(x, t)$, $x \in \Omega$. As $S_h \subset H^2(\Omega, \mathcal{T}_h)$ the previous forms have sense as well as for $u_h, \varphi_h \subset S_h$. Then we formulate the *discrete problem*: We define an approximate solution as a function u_h satisfying the conditions

$$\text{a) } u_h \in C^1([0, T], S_h), \quad (23)$$

$$\begin{aligned} \text{b) } \left(\frac{\partial u_h(t)}{\partial t}, \varphi_h \right) + b_h(u_h(t), \varphi_h) + a_h(u_h(t), \varphi_h) + J_h(u_h(t), \varphi_h) &= \ell_h(\varphi_h)(t) \\ &\quad \forall \varphi_h \in S_h \quad \forall t \in (0, T), \end{aligned}$$

$$\text{c) } u_h(0) = u_h^0,$$

where u_h^0 is an S_h -approximation of u^0 (e. g., L^2 -projection).

We have carried out the semidiscretization in space (called the *method of lines*) leading to a system of ordinary differential equations. In practical computations suitable time discretization is applied (Euler forward or backward scheme, Runge–Kutta methods or discontinuous Galerkin time discretization) and integrals are evaluated with the aid of numerical integration. The simplest time discretization is the Euler forward scheme. However, it suffers from a rather restrictive time step limitation due to a CFL-stability condition. Quite popular is therefore a *semimplicit scheme*, in which the nonlinear convective terms are treated explicitly, whereas the diffusion terms are approximated in an implicit way.

2.3 Numerical analysis

In [15], we investigate problem (1)–(4) with (6)–(7). Using some assumptions for triangulation and the numerical flux, we derive an apriori error estimation for the error

$$e_h \equiv u_h - u, \quad (24)$$

where u is the exact solution of (1)–(4), (6), (7) and u_h is its approximate solution given by (23).

Assumptions (T): Let us consider a system $\{\mathcal{T}_h\}_{h \in (0, h_0)}$, $h_0 > 0$, of partitions of the domain Ω ($\mathcal{T}_h = \{K_i\}_{i \in I_h}$, $I_h \subset \mathbb{Z}^+$) and assume that it has the following properties:

(T1) Each element $K \in \mathcal{T}_h$, $h \in (0, h_0)$ is *star-shaped* with respect to at least one point $x_K \in K$. We assume that

i) there exists a constant $\kappa > 0$ independent of K and h such that

$$\frac{\max_{x \in \partial K} |x - x_K|}{\min_{x \in \partial K} |x - x_K|} \leq \kappa \quad \forall K \in \mathcal{T}_h, h \in (0, h_0), \quad (25)$$

ii) element K has piecewise smooth Lipschitz boundary and K can be divided into a finite number of simplex

$$\overline{K} = \bigcup_{S \in \mathcal{S}(K)} \overline{S}, \quad (26)$$

there exists a positive constant c_1 such that

$$\frac{h_S}{\rho_S} \leq c_1 \quad \forall S \in \mathcal{S}(K) \quad (\text{shape regularity}), \quad (27)$$

where h_S is the diameter of S , ρ_S is the radius of the largest d -dimensional ball inscribed into S and moreover

$$0 < \frac{1}{\tilde{\kappa}} \leq \frac{h_K}{h_S} \leq \tilde{\kappa} < \infty \quad \forall S \in \mathcal{S}(K), \quad (28)$$

where h_K is the diameter of K and $\tilde{\kappa}$ is a constant independent of K and h .

(T2) There exists a constant $c_2 > 0$ such that

$$h_{K_i} \leq c_2 d(\Gamma_{ij}), \quad i \in I, j \in S(i), h \in (0, h_0). \quad (29)$$

Assumptions (T) admit very general elements, e.g., triangles, quadrilaterals, polygons, nonconvex elements and also elements not satisfying the usual conforming properties from the finite element method (elements with hanging nodes). These assumptions guarantee the validity of the multiplicative trace theorem and the inverse inequality, which are fundamental for the numerical analysis in [15].

Assumptions (H):

1. $H(u, v, \mathbf{n})$ is defined in $\mathbb{R}^d \times \mathcal{S}_1$, where $\mathcal{S}_1 = \{\mathbf{n} \in \mathbb{R}^d; |\mathbf{n}| = 1\}$, and *Lipschitz-continuous* with respect to u, v :

$$|H(u, v, \mathbf{n}) - H(u^*, v^*, \mathbf{n})| \leq c_3(|u - u^*| + |v - v^*|), \quad (30)$$

$$u, v, u^*, v^* \in \mathbb{R}, \mathbf{n} \in \mathcal{S}_1.$$

2. $H(u, v, \mathbf{n})$ is *consistent*:

$$H(u, u, \mathbf{n}) = \sum_{s=1}^d f_s(u) n_s, \quad u \in \mathbb{R}, \mathbf{n} = (n_1, \dots, n_d) \in \mathcal{S}_1. \quad (31)$$

3. $H(u, v, \mathbf{n})$ is *conservative*:

$$H(u, v, \mathbf{n}) = -H(v, u, -\mathbf{n}), \quad u, v \in \mathbb{R}, \mathbf{n} \in \mathcal{S}_1. \quad (32)$$

Now, we formulate the main theoretical result:

Theorem 2.1 *Let assumptions (T) and (H) be satisfied. Let u be the exact strong solution of problem (1) – (4), (6), (7) satisfying*

$$u \in L^2(0, T; H^{p+1}(\Omega)), \quad \frac{\partial u}{\partial t} \in L^2(0, T; H^{p+1}(\Omega)), \quad (33)$$

where the integer number $p \geq 1$ is a given degree of approximation. Let u_h be the approximate solution defined by (23). Then the error $e_h = u_h - u$ satisfies the estimate

$$\begin{aligned} & \sup_{t \in [0, T]} \|e_h(t)\|_{L^2(\Omega)}^2 + \varepsilon \int_0^T (|e_h(\vartheta)|_{H^1(\Omega, \tau_h)}^2 + J_h^\sigma(e_h(\vartheta), e_h(\vartheta))) \, d\vartheta \\ & + C_1(1 + \varepsilon) \int_0^T \left\{ \exp\left(C_1 \frac{1 + \varepsilon}{\varepsilon}(T - \vartheta)\right) \right. \\ & \quad \left. \times \left[\int_0^\vartheta (|e_h(\alpha)|_{H^1(\Omega, \tau_h)}^2 + J_h^\sigma(e_h(\alpha), e_h(\alpha))) \, d\alpha \right] \right\} \, d\vartheta \\ & \leq 2h^{2p} \left\{ \left(\frac{C_4(\varepsilon^2 + h^2)}{\varepsilon} + c_2 + \varepsilon C_3 \right) \exp\left(C_1 \frac{1 + \varepsilon}{\varepsilon} T\right) + C_2 \right\}, \end{aligned} \quad (34)$$

with constants $C_1, \dots, C_4 > 0$ independent of h and ε and c_2 is the constant from (29).

Proof: See [15].

Remark 2.2 This error estimate is not optimal as we have only first order of convergence for piecewise linear approximation ($p = 1$). On the other hand, the numerical examples carried out in [15] gives the computational order of convergence equal to 2 for $p = 1$.

3 SYSTEM OF THE NAVIER-STOKES EQUATIONS

In this section, we extend the approach explained above to the system of equations, particularly to the compressible Navier–Stokes equations. For simplicity, we shall consider 2-dimensional problems, i.e., we assume that $d = 2$.

3.1 Governing equations

Let $\Omega \subset \mathbb{R}^2$ be a bounded domain and $T > 0$. We set $Q_T = \Omega \times (0, T)$ and by $\partial\Omega$ denote the boundary of Ω which consists of several disjoint parts. We distinguish inlet Γ_I , outlet Γ_O and impermeable walls Γ_W on $\partial\Omega$. The system of the compressible Navier–Stokes equations describing 2D viscous flow can be written in the dimensionless form

$$\frac{\partial \mathbf{w}}{\partial t} + \sum_{s=1}^2 \frac{\partial \mathbf{f}_s(\mathbf{w})}{\partial x_s} = \sum_{s=1}^2 \frac{\partial \mathbf{R}_s(\mathbf{w}, \nabla \mathbf{w})}{\partial x_s} \quad \text{in } Q_T, \quad (35)$$

where

$$\mathbf{w} = (w_1, \dots, w_4)^T = (\rho, \rho v_1, \rho v_2, e)^T \quad (36)$$

is the so-called *state vector*,

$$\begin{aligned} \mathbf{f}_s(\mathbf{w}) &= (f_s^{(1)}(\mathbf{w}), \dots, f_s^{(4)}(\mathbf{w}))^T \\ &= (\rho v_s, \rho v_s v_1 + \delta_{s1} p, \rho v_s v_2 + \delta_{s2} p, (e + p) v_s)^T, \quad s = 1, 2, \end{aligned} \quad (37)$$

are the so-called *inviscid (Euler) fluxes* and

$$\begin{aligned} \mathbf{R}_s(\mathbf{w}, \nabla \mathbf{w}) &= (R_s^{(1)}(\mathbf{w}, \nabla \mathbf{w}), \dots, R_s^{(4)}(\mathbf{w}, \nabla \mathbf{w}))^T \\ &= \left(0, \tau_{s1}, \tau_{s2}, \sum_{k=1}^2 \tau_{sk} v_k + \frac{\gamma}{Re Pr} \frac{\partial \theta}{\partial x_s} \right)^T, \quad s = 1, 2, \end{aligned} \quad (38)$$

are the so-called *viscous fluxes*. We consider the Newtonian type of fluid, i.e., the viscous part of the stress tensor has the form

$$\tau_{sk} = \frac{1}{Re} \left[\left(\frac{\partial v_s}{\partial x_k} + \frac{\partial v_k}{\partial x_s} \right) - \frac{2}{3} \operatorname{div}(\mathbf{v}) \delta_{sk} \right], \quad s, k = 1, 2. \quad (39)$$

We use the following notation: ρ – density, p – pressure, e – total energy, $\mathbf{v} = (v_1, v_2)$ – velocity, θ – temperature, γ – Poisson adiabatic constant, Re – Reynolds number, Pr – Prandtl number.

In order to close the system we consider the following thermodynamical relations: the state equation for perfect gas and the relation for total energy

$$p = (\gamma - 1)(e - \rho|\mathbf{v}|^2/2), \quad e = c_V \rho \theta + \rho|\mathbf{v}|^2/2, \quad (40)$$

where c_V is the specific heat at constant volume which is equal to one in the dimensionless case. The system (35) – (40) is *hyperbolic-parabolic* type. It is equipped with the initial condition

$$\mathbf{w}(x, 0) = \mathbf{w}^0(x), \quad x \in \Omega, \quad (41)$$

and the following set of boundary conditions on appropriate parts of boundary:

$$\begin{aligned} a) \quad & \rho = \rho_D, \quad \mathbf{v} = \mathbf{v}_D, \quad \sum_{k=1}^2 \left(\sum_{l=1}^2 \tau_{lk} n_l \right) v_k + \frac{\gamma}{Re Pr} \frac{\partial \theta}{\partial \mathbf{n}} = 0 \quad \text{on } \Gamma_I, \\ b) \quad & \sum_{k=1}^2 \tau_{sk} n_k = 0, \quad s = 1, 2, \quad \frac{\partial \theta}{\partial \mathbf{n}} = 0 \quad \text{on } \Gamma_O, \\ c) \quad & \mathbf{v} = 0, \quad \frac{\partial \theta}{\partial \mathbf{n}} = 0 \quad \text{on } \Gamma_W, \end{aligned} \quad (42)$$

where ρ_D and \mathbf{v}_D are given function and $\mathbf{n} = (n_1, n_2)$ is a unit outer normal to $\partial\Omega$. Another possibility is to replace the adiabatic boundary condition (42), c) by

$$c') \quad \mathbf{v} = 0, \quad \theta = \theta_D \quad \text{on } \Gamma_W. \quad (43)$$

The problem to solve the compressible Navier-Stokes equations, equipped with the above initial and boundary conditions will be denoted by (CFP) (compressible flow problem).

The viscous terms $\mathbf{R}_s(\mathbf{w}, \nabla \mathbf{w})$ can be expressed in the form

$$\mathbf{R}_s(\mathbf{w}, \nabla \mathbf{w}) = \sum_{k=1}^2 \mathbf{K}_{sk}(\mathbf{w}) \frac{\partial \mathbf{w}}{\partial x_k}, \quad s = 1, \dots, 2, \quad (44)$$

where \mathbf{K}_{sk} are 2×2 matrices dependent on \mathbf{w} , see, e.g., [26].

3.2 DG FE formulation

In the discretization of (CFP) we proceed in a similar way as in Section 2.2. The approximate solution \mathbf{w}_h as well as test functions φ_h are elements of the finite dimensional space of vector-valued functions

$$\mathbf{S}_h = S_h^4, \quad (45)$$

where $S_h = S^{p, -1}(\Omega, \mathcal{T}_h)$ is introduced in (12). By $\gamma_D(i)$ we now denote the index set of $j \in \gamma(i)$ where the Dirichlet boundary condition is prescribed on the face $\Gamma_{ij} \subset \partial\Omega$ for at least one component of \mathbf{w} .

Assuming that \mathbf{w} is a classical sufficiently regular solution of (CFP) and $\varphi \in H^2(\Omega, \mathcal{T}_h)^4$, we multiply equation (35) by φ , integrate over $K_i \in \mathcal{T}_h$, apply Green's theorem, sum over all $K_i \in \mathcal{T}_h$ and arrive at the identity

$$\begin{aligned} \int_{\Omega} \frac{\partial \mathbf{w}}{\partial t} \cdot \varphi \, dx &+ \sum_{i \in I} \left\{ \sum_{j \in s(i)} \int_{\Gamma_{ij}} \sum_{s=1}^2 \mathbf{f}_s(\mathbf{w}) (n_{ij})_s \cdot \varphi|_{\Gamma_{ij}} \, dS \right. \\ &- \int_{K_i} \sum_{s=1}^2 \mathbf{f}_s(\mathbf{w}) \cdot \frac{\partial \varphi}{\partial x_s} \, dx + \int_{K_i} \sum_{s=1}^2 \mathbf{R}_s(\mathbf{w}, \nabla \mathbf{w}) \cdot \frac{\partial \varphi}{\partial x_s} \, dx \\ &- \sum_{\substack{j \in s(i) \\ j < i}} \int_{\Gamma_{ij}} \sum_{s=1}^2 \langle \mathbf{R}_s(\mathbf{w}, \nabla \mathbf{w}) \rangle (n_{ij})_s \cdot [\varphi] \, dS \\ &\left. - \sum_{j \in \gamma(i)} \int_{\Gamma_{ij}} \sum_{s=1}^2 \mathbf{R}_s(\mathbf{w}, \nabla \mathbf{w}) (n_{ij})_s \cdot \varphi \, dS \right\} = 0. \end{aligned} \quad (46)$$

The extension of DGFEM from the scalar equation to the Navier–Stokes system is not quite straightforward. It is caused by the fact that the viscous (i. e. diffusion) terms \mathbf{R}_s are nonlinear. Therefore, it is not possible to construct additional viscous (diffusion) terms as in (15) and (16) by a simple exchange of \mathbf{w} and φ , because the resulting form would not be linear with respect to the test functions φ . This problem is overcome by a *partial linearization* of the viscous fluxes \mathbf{R}_s . We consider two possibilities of the partial linearization of \mathbf{R}_s .

Representations (44) of \mathbf{R}_s , $s = 1, 2$ are already linear with respect to $\nabla \mathbf{w}$. This leads us to adding the following stabilization terms to the left-hand side of (46) (compare with (14)):

$$\begin{aligned} & \sum_{i \in I} \left\{ \sum_{\substack{j \in s(i) \\ j < i}} \int_{\Gamma_{ij}} \sum_{s=1}^2 \left\langle \sum_{k=1}^2 \mathbf{K}_{sk}(\mathbf{w}) \frac{\partial \varphi}{\partial x_k} \right\rangle (n_{ij})_s \cdot [\mathbf{w}] \, dS \right. \\ & \left. + \sum_{j \in \gamma_D(i)} \int_{\Gamma_{ij}} \sum_{s=1}^2 \sum_{k=1}^2 \mathbf{K}_{sk}(\mathbf{w}) \frac{\partial \varphi}{\partial x_k} (n_{ij})_s \cdot (\mathbf{w} - \mathbf{w}_B) \, dS \right\}, \end{aligned} \quad (47)$$

where \mathbf{K}_{sk} , $s, k = 1, 2$ were introduced in (44) and \mathbf{w}_B is a boundary state vector specified later. However, the numerical experiments indicate, that DGFEM scheme with the stabilization terms (47) is not stable. It is caused by the fact that whereas all diffusive terms in (46) are equal to zero for $\varphi = (\varphi_1, 0, 0, 0)$, $\varphi_1 \neq 0$, $\varphi_1 \in H^2(\Omega, \mathcal{T}_h)$ that the terms (47) are nonzero. Our goal is to replace (47) by stabilization terms which are linear with respect to $\varphi = (\varphi_1, \dots, \varphi_4)$ but independent of $\nabla \varphi_1$.

This partial linearization of the viscous terms $\mathbf{R}_s(\mathbf{w}, \nabla \mathbf{w})$ is obtained by the differentiation inside the definition of $\mathbf{R}_s(\mathbf{w}, \nabla \mathbf{w})$. Replacing the physical quantities ρ , \mathbf{v} and θ by the components of the state vector \mathbf{w} we have from (36), (38) and (39)

$$\mathbf{R}_1(\mathbf{w}, \nabla \mathbf{w}) = \begin{pmatrix} 0 \\ \frac{2}{3} \frac{1}{Re} \left(2 \frac{\partial}{\partial x_1} \left(\frac{w_2}{w_1} \right) - \frac{\partial}{\partial x_2} \left(\frac{w_3}{w_1} \right) \right) \\ \frac{1}{Re} \left(\frac{\partial}{\partial x_1} \left(\frac{w_3}{w_1} \right) + \frac{\partial}{\partial x_2} \left(\frac{w_2}{w_1} \right) \right) \\ \frac{w_2}{w_1} R_1^{(2)} + \frac{w_3}{w_1} R_1^{(3)} + \frac{\gamma}{Re Pr} \frac{\partial}{\partial x_1} \left(\frac{w_4}{w_1} - \frac{1}{2w_1^2} (w_2^2 + w_3^2) \right) \end{pmatrix}, \quad (48)$$

where $R_1^{(2)}$ and $R_1^{(3)}$ are the second and third component of $\mathbf{R}_1(\mathbf{w}, \nabla \mathbf{w})$, respectively, and

$$\mathbf{R}_2(\mathbf{w}, \nabla \mathbf{w}) = \begin{pmatrix} 0 \\ \frac{1}{Re} \left(\frac{\partial}{\partial x_1} \left(\frac{w_3}{w_1} \right) + \frac{\partial}{\partial x_2} \left(\frac{w_2}{w_1} \right) \right) \\ \frac{2}{3} \frac{1}{Re} \left(2 \frac{\partial}{\partial x_2} \left(\frac{w_3}{w_1} \right) - \frac{\partial}{\partial x_1} \left(\frac{w_2}{w_1} \right) \right) \\ \frac{w_2}{w_1} R_2^{(2)} + \frac{w_3}{w_1} R_2^{(3)} + \frac{\gamma}{Re Pr} \frac{\partial}{\partial x_2} \left(\frac{w_4}{w_1} - \frac{1}{2w_1^2} (w_2^2 + w_3^2) \right) \end{pmatrix}, \quad (49)$$

where $R_2^{(2)}$ and $R_2^{(3)}$ are the second and third component of $\mathbf{R}_2(\mathbf{w}, \nabla \mathbf{w})$, respectively. Performing the chain rule in the terms \mathbf{R}_s , $s = 1, 2$ we have

$$\mathbf{R}_1(\mathbf{w}, \nabla \mathbf{w}) = \begin{pmatrix} 0 \\ \frac{2}{3} \frac{1}{Re w_1} \left[2 \left(\frac{\partial w_2}{\partial x_1} - \frac{w_2}{w_1} \frac{\partial w_1}{\partial x_1} \right) - \left(\frac{\partial w_3}{\partial x_2} - \frac{w_3}{w_1} \frac{\partial w_1}{\partial x_2} \right) \right] \\ \frac{1}{Re w_1} \left[\left(\frac{\partial w_3}{\partial x_1} - \frac{w_3}{w_1} \frac{\partial w_1}{\partial x_1} \right) + \left(\frac{\partial w_2}{\partial x_2} - \frac{w_2}{w_1} \frac{\partial w_1}{\partial x_2} \right) \right] \\ \frac{w_2}{w_1} R_1^{(2)} + \frac{w_3}{w_1} R_1^{(3)} + \frac{\gamma}{Re Pr} \frac{1}{w_1} \times \\ \times \left[\frac{\partial w_4}{\partial x_1} - \frac{w_4}{w_1} \frac{\partial w_1}{\partial x_1} - \frac{1}{w_1} \left(w_2 \frac{\partial w_2}{\partial x_1} + w_3 \frac{\partial w_3}{\partial x_1} \right) + \frac{1}{w_1^2} (w_2^2 + w_3^2) \frac{\partial w_1}{\partial x_1} \right] \end{pmatrix}, \quad (50)$$

and

$$\mathbf{R}_2(\mathbf{w}, \nabla \mathbf{w}) = \begin{pmatrix} 0 \\ \frac{1}{Re w_1} \left[\left(\frac{\partial w_3}{\partial x_1} - \frac{w_3}{w_1} \frac{\partial w_1}{\partial x_1} \right) + \left(\frac{\partial w_2}{\partial x_2} - \frac{w_2}{w_1} \frac{\partial w_1}{\partial x_2} \right) \right] \\ \frac{2}{3} \frac{1}{Re w_1} \left[2 \left(\frac{\partial w_3}{\partial x_2} - \frac{w_3}{w_1} \frac{\partial w_1}{\partial x_2} \right) - \left(\frac{\partial w_2}{\partial x_1} - \frac{w_2}{w_1} \frac{\partial w_1}{\partial x_1} \right) \right] \\ \frac{w_2}{w_1} R_2^{(2)} + \frac{w_3}{w_1} R_2^{(3)} + \frac{\gamma}{Re Pr} \frac{1}{w_1} \times \\ \times \left[\frac{\partial w_4}{\partial x_2} - \frac{w_4}{w_1} \frac{\partial w_1}{\partial x_2} - \frac{1}{w_1} \left(w_2 \frac{\partial w_2}{\partial x_2} + w_3 \frac{\partial w_3}{\partial x_2} \right) + \frac{1}{w_1^2} (w_2^2 + w_3^2) \frac{\partial w_1}{\partial x_2} \right] \end{pmatrix}. \quad (51)$$

Now for $\mathbf{w} = (w_1, \dots, w_4)^\top$ and $\boldsymbol{\varphi} = (\varphi_1, \dots, \varphi_4)^\top$ we define the vector-valued functions

$$\mathbf{D}_1(\mathbf{w}, \nabla \mathbf{w}, \boldsymbol{\varphi}, \nabla \boldsymbol{\varphi}) \equiv \begin{pmatrix} 0 \\ \frac{2}{3} \frac{1}{Re w_1} \left[2 \left(\frac{\partial \varphi_2}{\partial x_1} - \frac{\varphi_2}{w_1} \frac{\partial w_1}{\partial x_1} \right) - \left(\frac{\partial \varphi_3}{\partial x_2} - \frac{\varphi_3}{w_1} \frac{\partial w_1}{\partial x_2} \right) \right] \\ \frac{1}{Re w_1} \left[\left(\frac{\partial \varphi_3}{\partial x_1} - \frac{\varphi_3}{w_1} \frac{\partial w_1}{\partial x_1} \right) + \left(\frac{\partial \varphi_2}{\partial x_2} - \frac{\varphi_2}{w_1} \frac{\partial w_1}{\partial x_2} \right) \right] \\ \times \left[\frac{\partial \varphi_4}{\partial x_1} - \frac{\varphi_4}{w_1} \frac{\partial w_1}{\partial x_1} - \frac{1}{w_1} \left(w_2 \frac{\partial \varphi_2}{\partial x_1} + w_3 \frac{\partial \varphi_3}{\partial x_1} \right) + \frac{1}{w_1^2} (w_2 \varphi_2 + w_3 \varphi_3) \frac{\partial w_1}{\partial x_1} \right] \end{pmatrix}, \quad (52)$$

and

$$\mathbf{D}_2(\mathbf{w}, \nabla \mathbf{w}, \boldsymbol{\varphi}, \nabla \boldsymbol{\varphi}) \equiv \begin{pmatrix} 0 \\ \frac{1}{Re w_1} \left[\left(\frac{\partial \varphi_3}{\partial x_1} - \frac{\varphi_3}{w_1} \frac{\partial w_1}{\partial x_1} \right) + \left(\frac{\partial \varphi_2}{\partial x_2} - \frac{\varphi_2}{w_1} \frac{\partial w_1}{\partial x_2} \right) \right] \\ \frac{2}{3} \frac{1}{Re w_1} \left[2 \left(\frac{\partial \varphi_3}{\partial x_2} - \frac{\varphi_3}{w_1} \frac{\partial w_1}{\partial x_2} \right) - \left(\frac{\partial \varphi_2}{\partial x_1} - \frac{\varphi_2}{w_1} \frac{\partial w_1}{\partial x_1} \right) \right] \\ \times \left[\frac{\partial \varphi_4}{\partial x_2} - \frac{\varphi_4}{w_1} \frac{\partial w_1}{\partial x_2} - \frac{1}{w_1} \left(w_2 \frac{\partial \varphi_2}{\partial x_2} + w_3 \frac{\partial \varphi_3}{\partial x_2} \right) + \frac{1}{w_1^2} (w_2 \varphi_2 + w_3 \varphi_3) \frac{\partial w_1}{\partial x_2} \right] \end{pmatrix}. \quad (53)$$

where $D_s^{(2)}$, $D_s^{(3)}$, $s = 1, 2$ are the second and third components of $\mathbf{D}_s(\mathbf{w}, \nabla \mathbf{w}, \boldsymbol{\varphi}, \nabla \boldsymbol{\varphi})$, respectively. Obviously, the forms \mathbf{D}_s are consistent with \mathbf{R}_s , i.e.,

$$\mathbf{D}_s(\mathbf{w}, \nabla \mathbf{w}, \mathbf{w}, \nabla \mathbf{w}) = \mathbf{R}_s(\mathbf{w}, \nabla \mathbf{w}) \quad \forall \mathbf{w}, \quad s = 1, 2. \quad (54)$$

Further, the forms $\mathbf{D}_s(\mathbf{w}, \nabla \mathbf{w}, \boldsymbol{\varphi}, \nabla \boldsymbol{\varphi})$, $s = 1, 2$ are linear with respect $\boldsymbol{\varphi}$ and $\nabla \boldsymbol{\varphi}$ and therefore they satisfy the assumption of linearity as the forms $R_s(u, \alpha)$, $s = 1, 2$ from the scalar case (1) and (4). Finally, the forms \mathbf{D}_s , $s = 1, 2$ are independent of $\nabla \varphi_1$.

Similarly as in the scalar case, we arrive at the definition of the following forms (compare with (18) – (21))

$$\begin{aligned} \mathbf{a}_h(\mathbf{w}, \boldsymbol{\varphi}) &= \sum_{K_i \in \mathcal{T}_h} \left\{ \int_{K_i} \sum_{s=1}^2 \mathbf{R}_s(\mathbf{w}, \nabla \mathbf{w}) \cdot \frac{\partial \boldsymbol{\varphi}}{\partial x_s} dx \right. \\ &\quad + \sum_{\substack{j \in S(i) \\ j < i}} \int_{\Gamma_{ij}} \sum_{s=1}^2 \left(\langle \mathbf{D}_s(\mathbf{w}, \nabla \mathbf{w}, \mathbf{w}, \nabla \mathbf{w}) \rangle (n_{ij})_s \cdot [\boldsymbol{\varphi}] \right. \\ &\quad \quad \quad \left. - \langle \mathbf{D}_s(\mathbf{w}, \nabla \mathbf{w}, \boldsymbol{\varphi}, \nabla \boldsymbol{\varphi}) \rangle (n_{ij})_s \cdot [\mathbf{w}] \right) dS \\ &\quad + \sum_{j \in \gamma_D(i)} \int_{\Gamma_{ij}} \sum_{s=1}^2 \left(\mathbf{D}_s(\mathbf{w}, \nabla \mathbf{w}, \mathbf{w}, \nabla \mathbf{w}) (n_{ij})_s \cdot \boldsymbol{\varphi} dS \right. \\ &\quad \quad \quad \left. - \mathbf{D}_s(\mathbf{w}, \nabla \mathbf{w}, \boldsymbol{\varphi}, \nabla \boldsymbol{\varphi}) (n_{ij})_s \cdot (\mathbf{w} - \mathbf{w}_B) \right) dS \left. \right\} \end{aligned} \quad (55)$$

(diffusion form),

$$\tilde{\mathbf{b}}_h(\mathbf{w}, \boldsymbol{\varphi}) = \sum_{i \in I} \left\{ \sum_{j \in S(i)} \int_{\Gamma_{ij}} \sum_{s=1}^2 \mathbf{f}_s(\mathbf{w}) n_s \cdot \boldsymbol{\varphi} dS - \int_{K_i} \sum_{s=1}^2 \mathbf{f}_s(\mathbf{w}) \cdot \frac{\partial \boldsymbol{\varphi}}{\partial x_s} dx \right\}. \quad (56)$$

(convective form), and

$$\mathbf{J}_h(\mathbf{w}, \boldsymbol{\varphi}) = \sum_{K_i \in \mathcal{T}_h} \left\{ \sum_{\substack{j \in S(i) \\ j < i}} \int_{\Gamma_{ij}} \sigma[\mathbf{w}] \cdot [\boldsymbol{\varphi}] dS + \sum_{j \in \gamma_D(i)} \int_{\Gamma_{ij}} \sigma(\mathbf{w} - \mathbf{w}_B) \cdot \boldsymbol{\varphi} dS \right\} \quad (57)$$

(interior and boundary penalty terms). The stabilization parameter σ is chosen as $\sigma|_{\Gamma_{ij}} = (|\Gamma_{ij}| Re)^{-1}$.

The set $\gamma_D(i)$ contains edges where the Dirichlet boundary condition is given for at least one component of $\mathbf{w} = (w_1, \dots, w_4)$, i.e., edges lying on Γ_I or Γ_W . We prescribe the boundary state $\mathbf{w}_B = ((w_B)_1, \dots, (w_B)_4)$ by

$$(w_B)_r = \begin{cases} (w_D)_r & \text{if } w_r \text{ is prescribed on } \partial\Omega \\ w_r & \text{otherwise,} \end{cases}, \quad r = 1, \dots, 4. \quad (58)$$

In particular, for the case (42) a)–c) we have

$$\begin{aligned} \mathbf{w}_B &= (\rho|_{\Gamma_W}, 0, 0, \rho|_{\Gamma_W}\theta|_{\Gamma_W}) \text{ on } \Gamma_W, \\ \mathbf{w}_B &= (\rho_D, \rho_D(\mathbf{v}_D)_1, \rho_D(\mathbf{v}_D)_2, \rho|_{\Gamma_I}\theta|_{\Gamma_I} + \frac{1}{2}\rho_D|\mathbf{v}_D|^2) \text{ on } \Gamma_I, \end{aligned} \quad (59)$$

and for the case (42) a)–b), (43) c')

$$\begin{aligned} \mathbf{w}_B &= (\rho|_{\Gamma_W}, 0, 0, \rho|_{\Gamma_W}\theta_D) \text{ on } \Gamma_W, \\ \mathbf{w}_B &= (\rho_D, \rho_D(\mathbf{v}_D)_1, \rho_D(\mathbf{v}_D)_2, \rho|_{\Gamma_I}\theta|_{\Gamma_I} + \frac{1}{2}\rho_D|\mathbf{v}_D|^2) \text{ on } \Gamma_I, \end{aligned} \quad (60)$$

where ρ_D , \mathbf{v}_D and θ_D are given functions from the boundary conditions (42)–(43) and $\rho|_{\Gamma}$ and $\theta|_{\Gamma}$ are the values of density and temperature extrapolated from interior of Ω on the appropriate boundary part Γ , respectively.

Let $\mathbf{w}(t)$ denotes the function on Ω such that $\mathbf{w}(t)(x) = \mathbf{w}(x, t)$, $x \in \Omega$. Then with the aid of (46), (55) – (57) the DGFE formulation for the Navier-Stokes equations reads

$$\begin{aligned} \frac{d}{dt}(\mathbf{w}(t), \boldsymbol{\varphi}) &= \mathbf{a}_h(\mathbf{w}(t), \boldsymbol{\varphi}) + \tilde{\mathbf{b}}_h(\mathbf{w}(t), \boldsymbol{\varphi}) + \mathbf{J}_h(\mathbf{w}(t), \boldsymbol{\varphi}), \\ \mathbf{w}(t), \boldsymbol{\varphi} &\in H^2(\Omega, \mathcal{T}_h)^4, \quad t \in (0, T). \end{aligned} \quad (61)$$

Relation (61) represents a weak form of the Navier-Stokes equations in the sense of the broken Sobolev space introduced in (10).

3.3 Numerical solution

In order to proceed from (61) to the numerical scheme for the system of equations, we use the same strategy as for the scalar equation in Section 2.2. The relation (61) has sense for $\mathbf{w}_h(t), \boldsymbol{\varphi}_h \in \mathbf{S}_h$, $t \in (0, T)$.

The boundary integrals in (56) are approximated by the approach common in the finite volume method:

$$\int_{\Gamma_{ij}} \sum_{s=1}^2 \mathbf{f}_s(\mathbf{w}_h(t)) n_s \boldsymbol{\varphi}_h \, dS \approx \int_{\Gamma_{ij}} \mathbf{H}(\mathbf{w}_h|_{\Gamma_{ij}}(x, t), \mathbf{w}_h|_{\Gamma_{ji}}(x, t), \mathbf{n}_{ij}(x)) \boldsymbol{\varphi}_h|_{\Gamma_{ij}}(x) \, dS, \quad (62)$$

where \mathbf{H} is the numerical flux, $\mathbf{w}|_{\Gamma_{ij}}(x, \cdot)$ and $\mathbf{w}|_{\Gamma_{ji}}(x, \cdot)$ are the values of \mathbf{w} at $x \in \Gamma_{ij}$ considered from interior and exterior of K_i , respectively. We use the numerical flux based on the direct solution of the local Riemann problem, see [16], [33].

If $\Gamma_{ij} \subset \partial\Omega_h$, then there is no neighbour K_j of K_i adjacent to Γ_{ij} and the values of $\mathbf{w}_h|_{\Gamma_{ji}}$ must be determined on the basis of “inviscid” boundary conditions. We put $\mathbf{v} \cdot \mathbf{n} = 0$ on Γ_W and on Γ_I and Γ_O we consider the boundary conditions in such a way that the linearized system of the Euler equations is well-posed. It means that we prescribe m_n components of \mathbf{w} , and the other components are extrapolated from interior of Ω . Here m_n is the number of negative eigenvalues of the Jacobi matrix

$$\sum_{s=1}^2 \frac{D\mathbf{f}_s(\mathbf{w})}{D\mathbf{w}} n_s. \quad (63)$$

For more detail see [20], [26], [33].

Then the convective form \mathbf{b}_h is approximated by

$$\mathbf{b}_h(\mathbf{w}, \boldsymbol{\varphi}) = \sum_{i \in I} \left\{ \sum_{j \in S(i)} \int_{\Gamma_{ij}} \mathbf{H}(\mathbf{w}|_{\Gamma_{ij}}, \mathbf{w}|_{\Gamma_{ji}}, \mathbf{n}_{ij}) \cdot \boldsymbol{\varphi} \, dS - \int_{K_i} \sum_{s=1}^2 \mathbf{f}_s(\mathbf{w}) \cdot \frac{\partial \boldsymbol{\varphi}}{\partial x_s} \, dx \right\}. \quad (64)$$

Now we are ready to define a the DGFE numerical solution of the Navier-Stokes equations. We say that \mathbf{w}_h is an *approximate solution* of (61), if it satisfies the conditions

$$\begin{aligned} \text{a)} \quad & \mathbf{w}_h \in C^1([0, T], \mathbf{S}_h), \\ \text{b)} \quad & \frac{d}{dt} (\mathbf{w}_h(t), \boldsymbol{\varphi}_h) = \mathbf{a}_h(\mathbf{w}_h(t), \boldsymbol{\varphi}_h) + \mathbf{b}_h(\mathbf{w}_h(t), \boldsymbol{\varphi}_h) + \mathbf{J}_h(\mathbf{w}_h(t), \boldsymbol{\varphi}_h), \\ & \forall \boldsymbol{\varphi}_h \in \mathbf{S}_h \quad \forall t \in (0, T), \\ \text{c)} \quad & \mathbf{w}_h(0) = \mathbf{w}_h^0. \end{aligned} \tag{65}$$

The relations (65) represent a system of ordinary differential equations which can be solved by a suitable numerical method.

Remark 3.1 If the viscous flow effects are negligible ($Re \rightarrow \infty$) then $\mathbf{a}_h \equiv 0$ and $\mathbf{J}_h \equiv 0$. Therefore (65), b) reads to DGFE scheme for the Euler equations

$$\frac{d}{dt} (\mathbf{w}_h(t), \boldsymbol{\varphi}_h) = \mathbf{b}_h(\mathbf{w}_h(t), \boldsymbol{\varphi}_h) \quad \forall \boldsymbol{\varphi}_h \in \mathbf{S}_h \quad \forall t \in (0, T). \tag{66}$$

For a piecewise constant approximation ($p = 0$ in (45)) scheme (66) is identical with the finite volume method for the Euler equations. From this point of view we can consider DGFEM as a generalization of FVM.

3.4 Implementation

The numerical computations in this paper were realized over regular triangular grids with the aid of piecewise linear approximations. Based on the numerical examples carried out in [15] for a scalar nonlinear convection-diffusion equation and the results from [18] where DGFEM was applied for the inviscid flow simulation, we deduce that (65) is a second order method. A comparison of DGFEM with a first order scheme in [17] underlines this assertion.

We use the basis of $\mathbf{S}_h := S^{1,-1}$ whose components are piecewise linear functions associated with midpoints of sides of triangles:

$$\{\phi_{ij} \in \mathbf{S}_h; \phi_{ij}(Q_{kl}) = \delta_{ik}\delta_{jl}, \quad j \in S(i), \quad l \in S(k), \quad i, k \in I\}, \tag{67}$$

where Q_{kl} is the midpoint of Γ_{kl} . This choice leads to a diagonal mass matrix in (65), b). For the evaluation of boundary integrals in (55), (57) and (64), we use the two point Gauss quadrature rule

$$\int_{-1}^1 g(t) dt \approx g\left(-\frac{1}{\sqrt{3}}\right) + g\left(\frac{1}{\sqrt{3}}\right), \tag{68}$$

which is exact for polynomials of the third degree. The volume integrals in (55) and (64) are evaluated by the three point integration rule

$$\int_{K_i} g(x) dx \approx |K_i| \frac{1}{3} \sum_{j \in S(i)} g(Q_{ij}), \tag{69}$$

which is exact for second degree polynomials.

The systems of ordinary differential equations (65) can be solved by the two steps Runge-Kutta method which guarantees the accuracy with respect to the time coordinate. However, the use of the explicit scheme requires a restriction on a time step. Based on heuristic consideration and a number of numerical experiments we use the stability condition in the form

$$\Delta t = \frac{1}{3} CFL \min \left(\frac{1}{2} \max_{\substack{K_i \in T_h \\ j \in S(i)}} \left(\frac{|K_i|}{\lambda_{ij} |\Gamma_{ij}|} \right), \frac{1}{8} \max_{K_i \in T_h} \frac{Re}{|K_i|} \right), \tag{70}$$

where we put usually $CFL = 0.4$ and λ_{ij} is the maximal eigenvalue of the Jacobi matrix (63) evaluated over Γ_{ij} .

As the stability condition (70) is too restrictive the better approach is to use a suitable scheme for stiff systems. We employ CVODE code [10] which is based on a backward differential formula (BDF) method

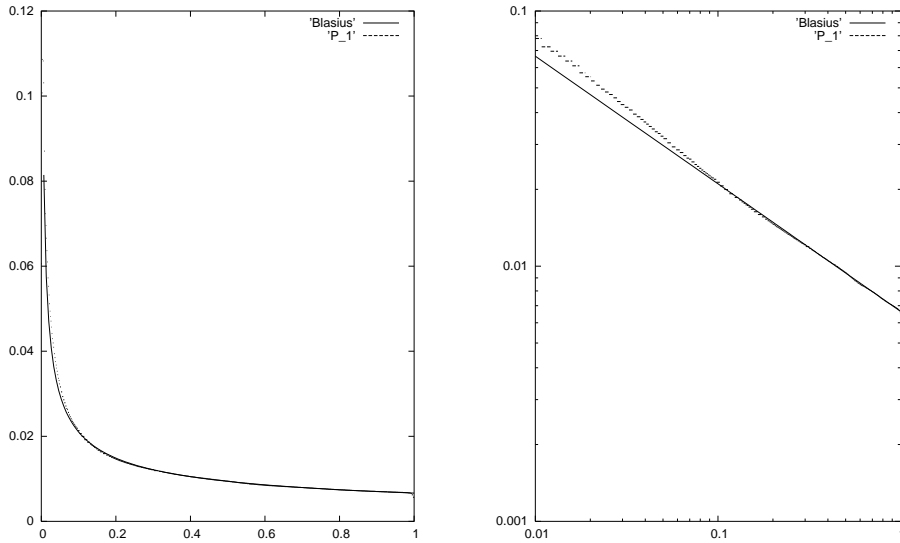


Fig. 1: Distribution of the computed skin friction coefficient (P_1) with the “theoretical” one (Blasius). The left and right figures are plotted in linear and logarithmic scaling, respectively

where the system of nonlinear equations is solved by a Newton method. The Jacobi matrix for Newton iterations is computed numerically.

In some cases the numerical solutions suffer from the so-called Gibbs effect, i.e., there are some overshoots and undershoots of a numerical solutions in vicinity of discontinuities (e. g., shock waves). In order to avoid this effect, an order limiting has to be applied. We use the order limiting based on the check of interelement jumps of the solution, see [19]. Moreover, in order to obtain physically relevant solution near nonpolygonal parts of boundary, we employ superparametric finite elements for triangles adjacent to a curved parts of boundary, see [13].

4 NUMERICAL EXAMPLES

We present several examples demonstrating the efficiency of DGFEM for the numerical simulation of compressible flows. We applied the time stabilization method in order to obtain steady state solutions. The used triangular grid were obtained by the anisotropic mesh adaptation method (AMA), see [11], [12]. The visualized isolines and distributions of quantities along boundaries are plotted without any postprocessing. Since we use a piecewise linear approximation, then isolines and distributions of the pressure coefficient are piecewise linear while distributions of skin friction coefficient are piecewise constant.

Examples 1 We consider the laminar flow on the adiabatic flat plate characterized by a freestream Mach number $M = 0.3$ and by a Reynolds number $Re = 10^4$. The computation has been performed on a unstructured grid having 3781 elements which was adaptive refined along the flat. Figure 1 shows the comparison of the computed skin friction coefficient c_f with the “theoretical” one which is given by the well-known Blasius formula for the c_f distribution along a flat plate for incompressible flow. The right figure represents the distribution plotted in logarithmic scale. The computed results show good agreement with the Blasius solution.

Examples 2 In the following examples we solve laminar viscous flows around the NACA0012 profile. In order to avoid the influence of an artificial external boundary we choose the computational domain Ω with diameter twenty times larger then the diameter of the profile.

The second example is a flow around the profile NACA0012 at free stream Mach number $M = 0.85$, an angle of attack $\alpha = 0^\circ$, Reynolds number $Re = 500$, and wall temperature is equal to the freestream total temperature.

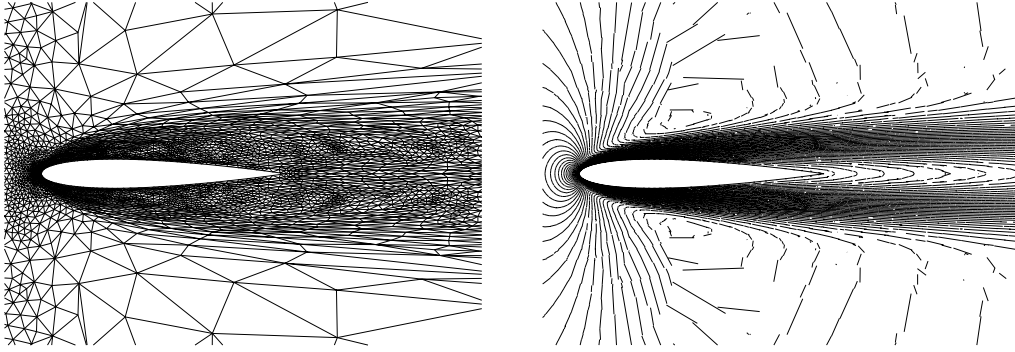


Fig. 2: Triangulation (left) and the corresponding Mach number isolines (right) around NACA0012 profile ($M = 0.85$, $\alpha = 0^\circ$, $Re = 500$)

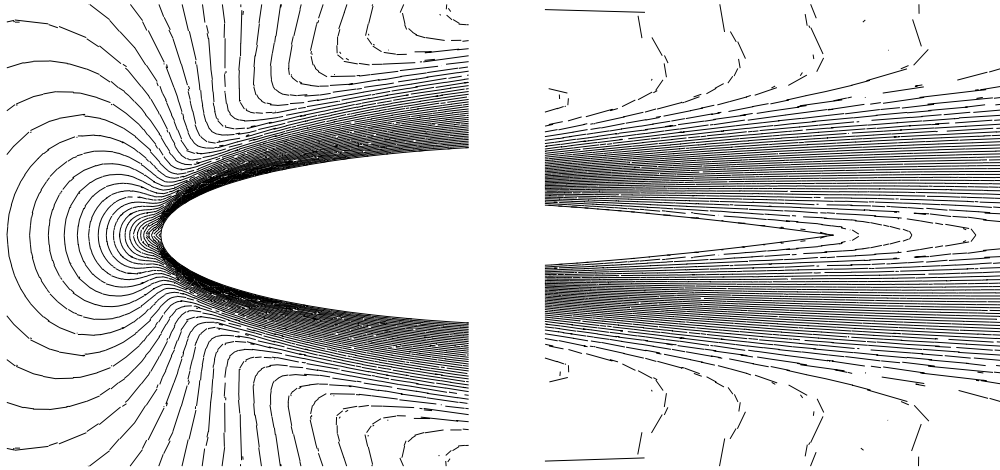


Fig. 3: Details of the Mach number isolines around the leading edge (left) and trailing edge (right) of NACA0012 profile ($M = 0.85$, $\alpha = 0^\circ$, $Re = 500$)

Figure 2 show the final triangulation obtain by AMA technique and the corresponding Mach number isolines (right). The details of Mach number isolines around the trailing and leading edges are shown in Figure 3. The pressure and skin friction distributions along the profile are plotted in Figure 4. Our computed value the drag coefficient is $c_D = 0.2281$ whereas the reference value from [28] is $c_D = 0.2230$.

Examples 3 In this example we consider a supersonic flow at free stream Mach number $M = 2$, an angle of attack $\alpha = 10^\circ$, Reynolds number $Re = 500$ and wall temperature is equal to the freestream total temperature. A characteristic feature of this flow problem is the presence of a detached bow shock wave in front of the profile. Figure 5 show the final triangulation obtain by AMA technique and the corresponding Mach number isolines (right). A sharp resolution of the bow shock wave is easily observed. The pressure and skin friction distributions along the profile are plotted in Figure 4. The computed values the drag and lift coefficients are $c_D = 0.2312$ and and $c_L = 0.3738$, respectively.

Examples 4 The last example is a flow around the profile NACA0012 at free stream Mach number $M = 0.5$, an angle of attack $\alpha = 0^\circ$, and Reynolds number $Re = 5000$. The walls of the profile are adiabatic. The Reynolds number is near to the upper limit for steady laminar flow. A characteristic

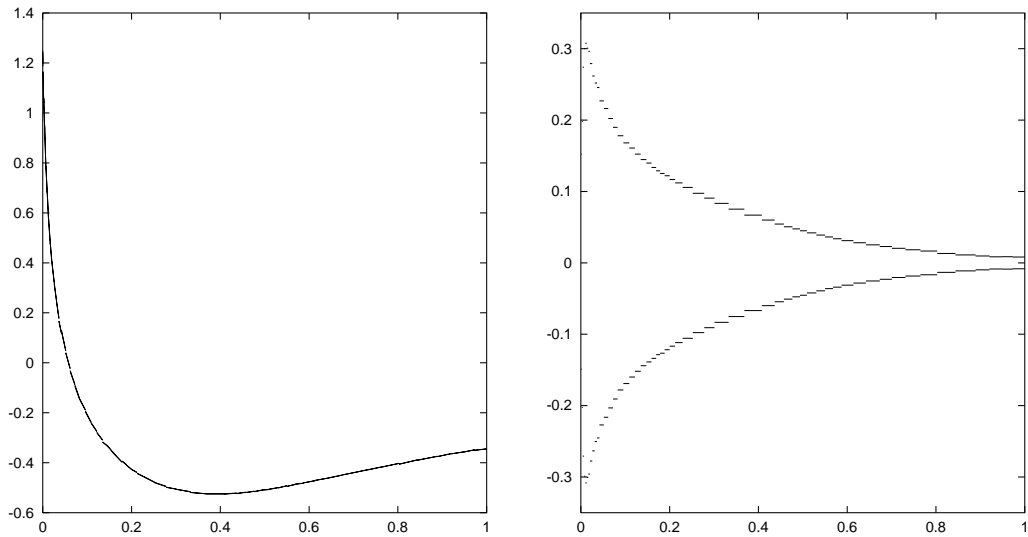


Fig. 4: Distributions of the pressure coefficient (left) and skin friction coefficient (right) along NACA0012 profile ($M = 0.85$, $\alpha = 0^\circ$, $Re = 500$)

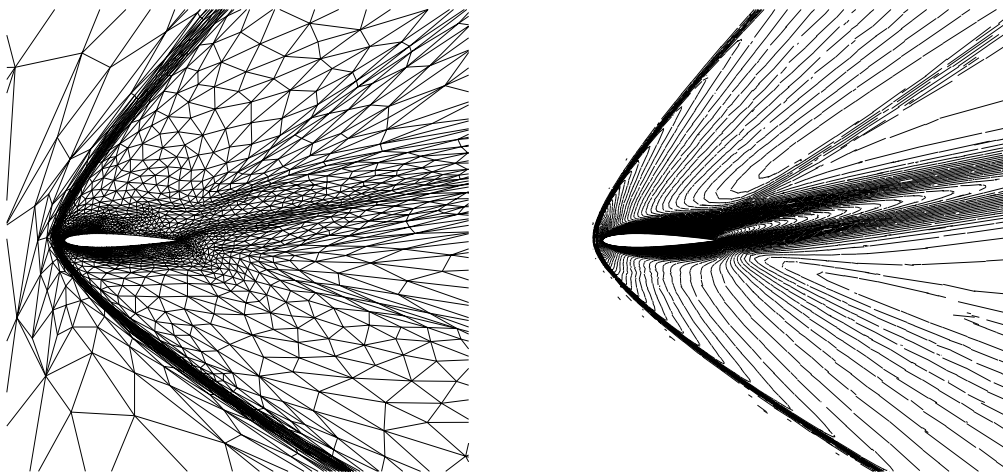


Fig. 5: Triangulation (left) and the corresponding Mach number isolines (right) around NACA0012 profile ($M = 2$, $\alpha = 10^\circ$, $Re = 500$)

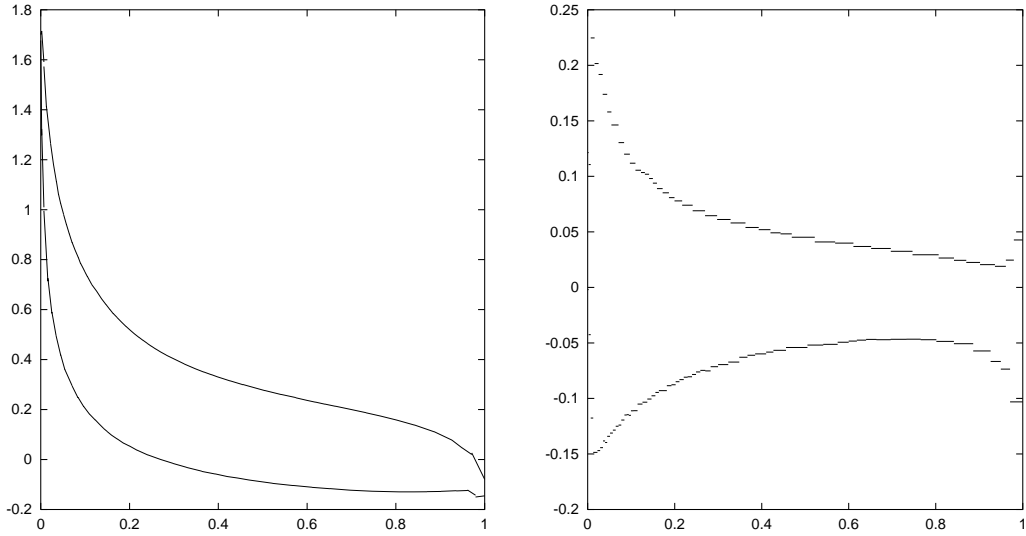


Fig. 6: Distributions of the pressure coefficient (left) and skin friction coefficient (right) along NACA0012 profile ($M = 2$, $\alpha = 10^\circ$, $Re = 500$)

method	$c_{D,p}$	$c_{D,v}$	c_D
DGFEM	0.02309	0.03113	0.05422
[28]	0.02281	0.03246	0.05527
[5] - P_1	0.01963	0.03051	0.05014
[5] - P_2	0.01991	0.03361	0.05352
[5] - P_3	0.02208	0.03303	0.05511

Tab. 1: Computed values of $c_{D,p}$, $c_{D,v}$ and c_D by the presented DGFEM in comparison with [28] and [5], piecewise linear (P_1), quadratic (P_2) and cubic approximation (P_3)

feature of this flow problem is the separation of the flow occurring near to the trailing edge.

Figure 7 show the final triangulation obtain by AMA technique and the corresponding Mach number isolines (right). The details of Mach number isolines around the trailing and leading edges are shown in Figure 8. The pressure and skin friction distributions along the profile are plotted in Figure 9. Table 1 shows the computed values the pressure part ($c_{D,p}$) and viscous part ($c_{D,v}$) of the drag coefficient in comparison with reference values from [28] and [5] where piecewise linear, quadratic and cubic DG approximation were applied. We observe good agreement with the reference results.

5 CONCLUSION

We present a new efficient numerical method for the solution of the compressible Navier-Stokes equations. The scheme presented is based on the discontinuous Galerkin finite element method with nonsymmetric treatment of diffusive stabilization terms and interior and boundary penalty. A special form of stabilization terms has been proposed and successfully tested. Several numerical examples demonstrate an accuracy and robustness of the method.

We implemented a piecewise linear approximation on unstructured triangular grids. An interesting observation is the following fact: although a discontinuous approximation is employed, the numerical solution looks continuous (i.e. interelement jumps are not visible) in subdomains where the solution is smooth. Work is in progress to implement a piecewise quadratic and cubic approximation and to simulate nonsteady problems.

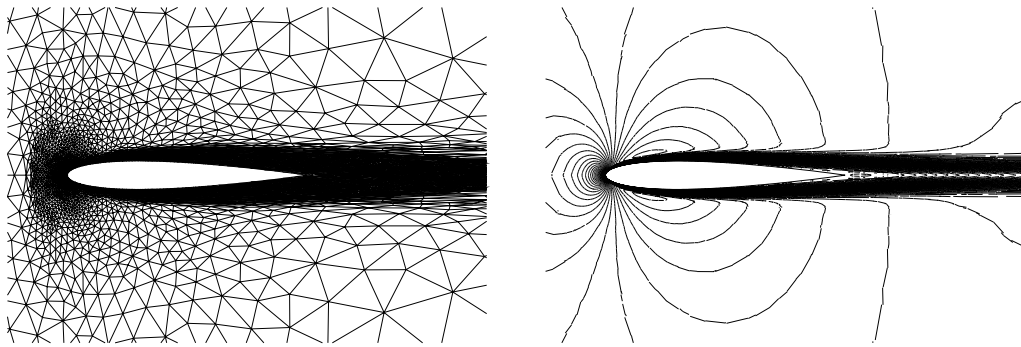


Fig. 7: Triangulation (left) and the corresponding Mach number isolines (right) around NACA0012 profile ($M = 0.5$, $\alpha = 0^\circ$, $Re = 5000$)

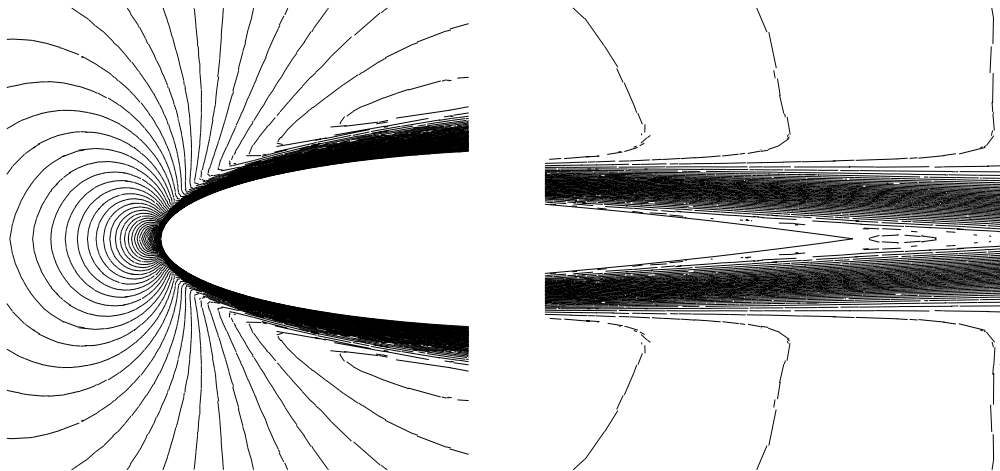


Fig. 8: Details of the Mach number isolines around the leading edge (left) and trailing edge (right) of NACA0012 profile ($M = 0.5$, $\alpha = 0^\circ$, $Re = 5000$)

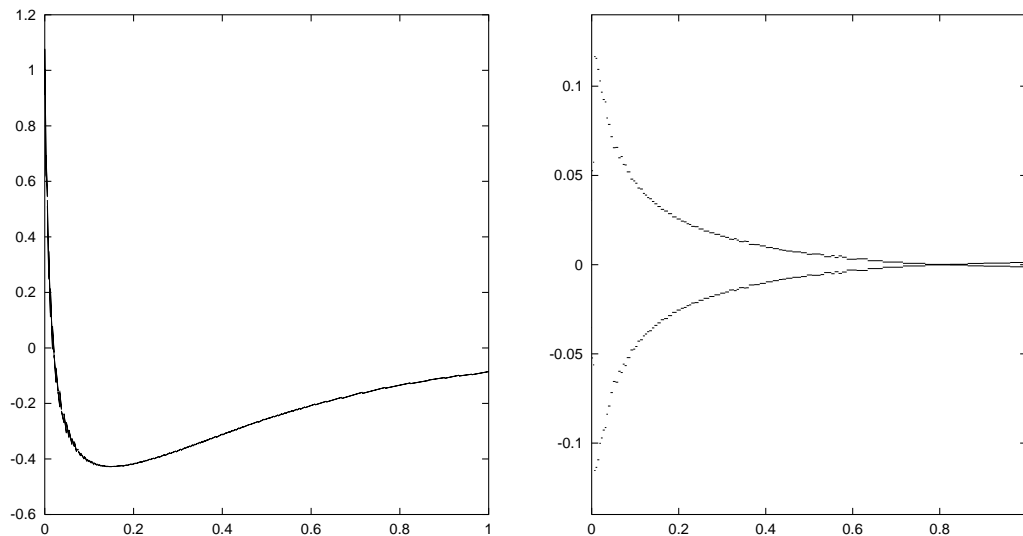


Fig. 9: Distributions of the pressure coefficient (left) and skin friction coefficient (right) along NACA0012 profile ($M = 0.5$, $\alpha = 0^\circ$, $Re = 5000$)

References

- [1] Abgrall R, Sonar T, Friedrich J, Billet G. Higher order approximations for compressible fluid dynamics on unstructured and cartesian meshes. In *High-Order Methods for Computational Physics, Lecture Notes in Computational Science and Engineering 9*, Barth TJ, Deconinck H (eds.) Springer, Berlin, 1999; 1–68.
- [2] Angot P, Dolejší V, Feistauer M, Felcman J. Analysis of a combined barycentric finite volume – nonconforming finite element method for nonlinear convection-diffusion problems. *Appl. Math.* 1998; **43**(4):263–310.
- [3] Babuška I, Zlámal M. Nonconforming elements in the finite element method with penalty. *SIAM J. Numer. Anal.* 1973; **10**:863–875.
- [4] Babuška I, Baumann CE, Oden JT. A discontinuous hp finite element method for diffusion problems: 1-d analysis. *Computers and Mathematics with Applications*, 1999; **37**:103–122.
- [5] Bassi F, Rebay S. A high-order accurate discontinuous finite element method for the numerical solution of the compressible Navier–Stokes equations. *J. Comput. Phys* 1997; **131**:267–279.
- [6] Bassi F, Rebay S. A high order discontinuous Galerkin method for compressible turbulent flow. In *Discontinuous Galerkin Method: Theory, Computations and Applications, Lecture Notes in Computational Science and Engineering 11*, Griebel M, Keyes DE, Nieminen RM, Rose D, Schlick T (eds). Springer-Verlag, 2000.
- [7] Baumann CE, Oden JT. A discontinuous hp finite element method for the Euler and Navier-Stokes equations. *Int. J. Numer. Methods Fluids* 1999; **31**(1):79–95.
- [8] Cockburn B. Discontinuous Galerkin methods for convection dominated problems. In *High-Order Methods for Computational Physics, Lecture Notes in Computational Science and Engineering 9*, Barth TJ, Deconinck H (eds.) Springer, Berlin, 1999; 69–224.
- [9] Cockburn B, Karniadakis GE, Shu CW. *Discontinuous Galerkin methods, Lecture Notes in Computational Science and Engineering 11.*, Springer, Berlin, 2000.
- [10] Cohen SD, Hindmarsh AC. *CVODE User Guide*. Lawrence Livermore National Laboratory, September 1994. <http://www.netlib.org/ode/cvode.tar.gz>.
- [11] Dolejší V. Anisotropic mesh adaptation for finite volume and finite element methods on triangular meshes. *Computing and Visualization in Science* 1998; **1**(3):165–178.
- [12] Dolejší V. Anisotropic mesh adaptation technique for viscous flow simulation. *East-West Journal of Numerical Mathematics* 2001; **9**(1):1–24.

- [13] Dolejší V, Feistauer M. On the discontinuous Galerkin method for the numerical solution of compressible high-speed flow. In *Numerical Mathematics and Advanced Applications, ENUMATH 2001*, Brezzi F, Buffa A, Corsaro S, Murli A (eds), Springer-Verlag, Italia, Milano, 2003; 65–84.
- [14] Dolejší V, Feistauer M, Schwab C. A finite volume discontinuous Galerkin scheme for nonlinear convection–diffusion problems. *Calcolo* 2002; **39**:1–40.
- [15] Dolejší V, Feistauer M, Sobotíková V. A discontinuous Galerkin method for nonlinear convection–diffusion problems. *Comput. Methods Appl. Mech. Eng.*, (submitted).
- [16] Dolejší V, Felcman J. Numerical methods for hyperbolic systems - application in fluid dynamics. *Engineering Mechanics* 2002; **9**(3):139–152.
- [17] Dolejší V. Discontinuous galerkin method for the compressible flow simulation. *C. R. Acad. Sci. Paris*, (submitted).
- [18] Dolejší V, Feistauer M. Semi-implicit discontinuous galerkin finite element method for the numerical solution of inviscid compressible flow. *J. Comput. Phys.*, (submitted).
- [19] Dolejší V, Feistauer M, Schwab C. On some aspects of the discontinuous Galerkin finite element method for conservation laws. *Math. Comput. Simul.* 2003; **61**:333–346.
- [20] Feistauer M. *Mathematical Methods in Fluid Dynamics*. Longman Scientific & Technical, Harlow, 1993.
- [21] Feistauer M, Felcman J. Theory and applications of numerical schemes for nonlinear convection-diffusion problems and compressible Navier–Stokes equations. In *The Mathematics of Finite Elements and Applications*, Whitemen JR (ed), John Wiley & Sons, 1996; 175–194.
- [22] Feistauer M, Felcman J, Dolejší V. Numerical simulation of compressible viscous flow through cascades of profiles. *ZAMM* 1996; **76**(S4):297–300.
- [23] Feistauer M, Felcman J, Lukáčová-Medvidová M. On the convergence of a combined finite volume – finite element method for nonlinear convection – diffusion problems. *Numer. Methods Partial Differ. Equations* 1997; **13**:163–190.
- [24] Feistauer M, Felcman J, Lukáčová-Medvidová M, Warnecke G. Error estimates of a combined finite volume – finite element method for nonlinear convection – diffusion problems. *SIAM J. Numer. Anal.* 1999; **36**(5):1528–1548.
- [25] Feistauer M, Felcman J, Lukáčová-Medvidová M. Combined finite element–finite volume solution of compressible flow. *J. Comput. Appl. Math.* 1995; **63**:179–199, 1995.
- [26] Feistauer M, Felcman J, Straškraba I. *Mathematical and Computational Methods for Compressible Flow*. Oxford University Press, Oxford, 2003.
- [27] Felcman J. Grid refinement–alignment in 3D flow computations. *Math. Comput. Simul.* 2003; **61**:317–331.
- [28] Khalfallah K, Lerat A. An efficient relaxation method for a centred Navier-Stokes solver. In *Numerical Methods for Fluid Dynamics V.*, Morton KW, Baines MJ (eds), Oxford Science Publications, 1995.
- [29] Lomtev I, Quillen CB, Karniadakis GE. Spectral/*hp* methods for viscous compressible flows on unstructured 2D meshes. *J. Comput. Phys* 1998, **144**:325–357.
- [30] Oden JT, Babuška I, Baumann CE. A discontinuous *hp* finite element method for diffusion problems. *J. Comput. Phys* 1998; **146**:491–519.
- [31] Rivière B, Wheeler MF, A discontinuous Galerkin method applied to nonlinear parabolic equations, In *Discontinuous Galerkin methods. Theory, computation and applications. Lecture Notes in Computational Science and Engineering 11*, Cockburn B et al (eds) Springer, Berlin, 2000; 231–244.
- [32] Shu CW. Higher order ENO and WENO schemes. unstructured and cartesian meshes. In *High-Order Methods for Computational Physics, Lecture Notes in Computational Science and Engineering 9*, Barth TJ, Deconinck H (eds) Springer, Berlin, 1999; 439–582.
- [33] Toro EF. *Riemann Solvers and Numerical Methods for Fluid Dynamics*. Springer-Verlag, 1997.